

MultiFocusing 3D diffraction imaging

A. Berkovitch (Geomage), K. Deev (Geomage), D. Pelman (Geomage) & M. Rauch-Davies* (Geomage)

Introduction

The detection of small scale geological objects such as faults, pinchouts, fractures, karsts etc. is an important challenge when applying seismic for hydrocarbon exploration. The wavefield generated by such subsurface elements is characterized by the presence of scattering or diffracted energy.

The amplitudes of diffracted waves are usually much weaker than those of specular reflections. Diffractions are essentially lost during the conventional processing/migration sequence, or they are masked in conventional seismic stacked sections. Local structural and lithological elements in the subsurface of a size comparable to the wavelength are usually ignored during processing and identified only during interpretation.

Efforts to image diffraction events were undertaken in Landa et al. (1987), Kanasevich and Phadke (1988), Landa and Keydar (1998) and Fomel et al. (2007), Moser and Harpen (2006), Berkovitch et al. (2009). Separation of diffracted and reflected wavefields based on different kinematic properties was proposed in Khaidukov et al. (2004). Taner et al. (2006), Klokov et al. (2011).

In this paper we present a generalization of the method proposed by Berkovitch et al. (2009) to 3D case. The method is based on MultiFocusing moveout time correction, which adequately describes not only reflection but also diffraction events. Optimal summation of the diffracted events and attenuation of the specular reflections allows creating an image containing mostly diffraction energy. We briefly describe the theory of the MultiFocusing method and demonstrate the efficiency of the proposed diffraction imaging technique on field data.

Moveout MultiFocusing correction for diffracted waves

The MultiFocusing method (MF) was proposed by Berkovitch et al. (1994) and it consists of constructing a zero-offset section wherein each trace of this section is computed from prestack traces arbitrarily located around an imaging position. The moveout correction does not require knowledge about the subsurface and is valid for arbitrary observation geometry. For a given source-receiver pair, the MF-moveout equations expresses the time shifts with respect to a zero-offset trace in terms of three parameters:

$$\Delta t = \frac{\sqrt{(R^+)^2 - 2R^+DX^+ \sin b + (DX^+)^2} - R^+}{V_0} + \frac{\sqrt{(R^-)^2 + 2R^-DX^- \sin b + (DX^-)^2} - R^-}{V_0}, \quad (1)$$

where

$$R^+ = \frac{1+S}{\frac{1}{R_{cee}} + \frac{S}{R_{cre}}}; \quad R^- = \frac{1-S}{\frac{1}{R_{cee}} - \frac{S}{R_{cre}}}; \quad (2)$$

$$\sigma = \frac{\Delta X^+ - \Delta X^-}{\Delta X^+ + \Delta X^- + 2 \frac{\Delta X^+ \Delta X^-}{R_{cre}} \sin \beta}. \quad (3)$$

In these equations, b is the normal ray; R_{cre} and R_{cee} are radii of curvatures of two paraxial wavefront: normal incident point wave and normal wave respectively; ΔX^+ and ΔX^- are the

source and receiver offsets for a given ray with respect to the central point X_0 ; R^+ and R^- are the radii of curvature of the fictitious waves defined by equations (2) and (3); V_0 is the near-surface velocity; and S is a focusing parameter.

Our goal here is to determine the time shift for any shot and receiver in the MultiFocusing super-gather near the central point X_0 . According to figure 1, the moveout correction for normal ray OX_0 for the trace corresponding to shot S and receiver R is given by

$$\Delta t = \frac{L_{SO} + L_{OR}}{V_0} - \frac{2R_{cre}}{V_0}, \quad (4)$$

Where

$$L_{SO} = \sqrt{(\Delta X^- + R_{cre} \sin \beta)^2 + (R_{cre} \cos \beta)^2} = \sqrt{R_{cre}^2 + 2\Delta X^- R_{cre} \sin \beta + (\Delta X^-)^2}; \quad (5)$$

$$L_{OR} = \sqrt{(\Delta X^+ - R_{cre} \sin \beta)^2 + (R_{cre} \cos \beta)^2} = \sqrt{R_{cre}^2 - 2\Delta X^+ R_{cre} \sin \beta + (\Delta X^+)^2}$$

Then

$$\Delta \tau = \frac{\sqrt{(R_{cre})^2 - 2R_{cre}\Delta X^+ \sin \beta_0 + (\Delta X^+)^2} - R_{cre}}{V_0} + \frac{\sqrt{(R_{cre})^2 + 2R_{cre}\Delta X^- \sin \beta_0 + (\Delta X^-)^2} - R_{cre}}{V_0} \quad (6)$$

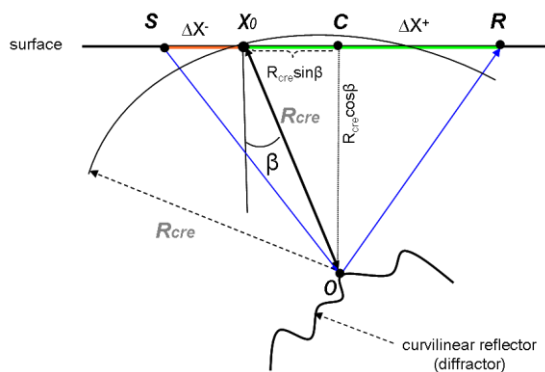


Figure 1. MultiFocusing ray diagram for diffracted wave detection.

As it follows from equation (6), diffraction moveout coincides with the MultiFocusing moveout when reflection interface shrinks to a point, i.e. when $R_{cre} = R_{cee}$.

Practical implementation of diffraction stacking is a special case of MultiFocusing. For diffraction stacking, however, only two parameters (for 2D case) should be searched, namely R_{cre} and β . In the 3D case there are 5 parameters to be estimated from the data: three curvatures and two emergence angles. The parameters are estimated by maximizing the semblance function calculated for all seismic traces in the super-gather. The result of the diffraction imaging is a time section containing mostly optimally stacked diffraction events and residual specular reflections. Such sections contain important information for identifying local heterogeneities and discontinuities in the subsurface.

In the MF method, the size of the summation aperture around the central point X_0 for reflected waves is defined by the equation (Hubral et al., 1993),

$$W = \frac{2}{\cos b} \sqrt{\frac{V_0 T}{2 \left| \frac{1}{R_{cee}} - \frac{1}{R_{cre}} \right|}} \quad (7)$$

where T is the period of the signal ($T = 1/f$, with f is a dominant frequency).

For diffracted waves, since $R_{cee} = R_{cre}$, and $W = \forall$. As such, theoretically it is possible to use an aperture of any size. This, however, is not justified in the presence of strongly varying geological conditions in the subsurface and strong attenuation of the diffracted energy. Therefore, for construction of the diffraction oriented stack, we choose an aperture (sources and receivers distances from the central point X_0) similar by value to migration aperture.

Real data example

We applied MF diffraction imaging on 3D seismic data from the Kazakhstan onshore. The dataset consists of 1800 in-lines and 450 cross-lines with bin size 25x25 meters. Source and receiver lines spaced 400 and 300 meters respectively with nominal fold of 50. In principle for each surface location and for each time sample we need to search three radius parameters ($R_{cre}^x, R_{cre}^y, R_{cre}^{xy}$) and two emergence angles (β_x, β_y). Since radius R_{cre} is connected to the RMS velocity in the medium our search was performed around a priori known RMS/migration velocity. Taking into consideration that migration can be regarded as summation over diffraction surfaces and assigning result to the diffraction apex we put angle values equal to zero. In this way we reduce number of searched parameters and obtain directly migrated diffraction images. Summation was performed according to the diffraction moveout correction (equation (6)).

Figure 2a shows un-migrated inline section. Numerous diffraction events can be observed in the central part of the section. Strongly faulted zones are shown by red circles. Figure 2b illustrates the same seismic line after post stack time migration. The diffraction events are now successfully focused and the red circles fit to the faulted zone. Figure 2c shows a MF diffraction image of the same in-line. The reflection events are strongly attenuated, leaving well-imaged diffraction events from the faulted zone (red circles). Strong diffraction energy at the left side of the bottom indicates a rough character of the reflected interface.

Conclusions

We are proposing a new algorithm of 3D diffraction imaging based on a multifocusing methodology. This method consists of optimal summation of seismic data in accordance with a diffraction-moveout formula. The diffraction-oriented stacked sections can be used for reliable interpretation of non-smoothed geological interfaces and for identification of local heterogeneities such as faults, carsts, fractures etc. We demonstrate this application for a 3D dataset.

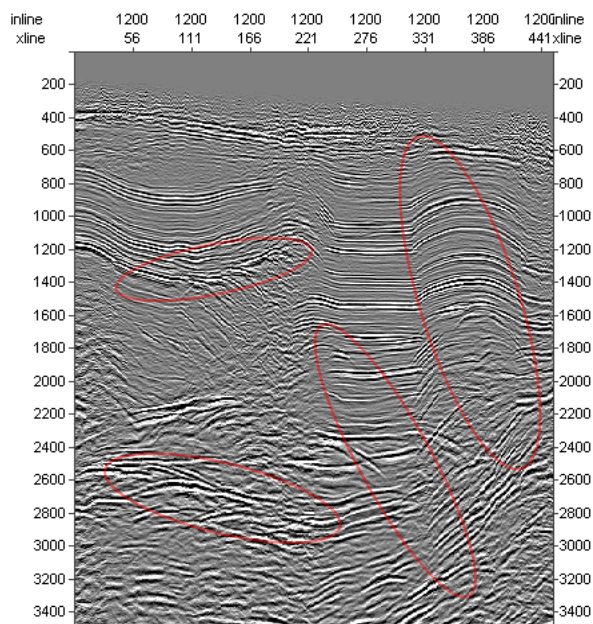


Figure 2(a). unmigrated section

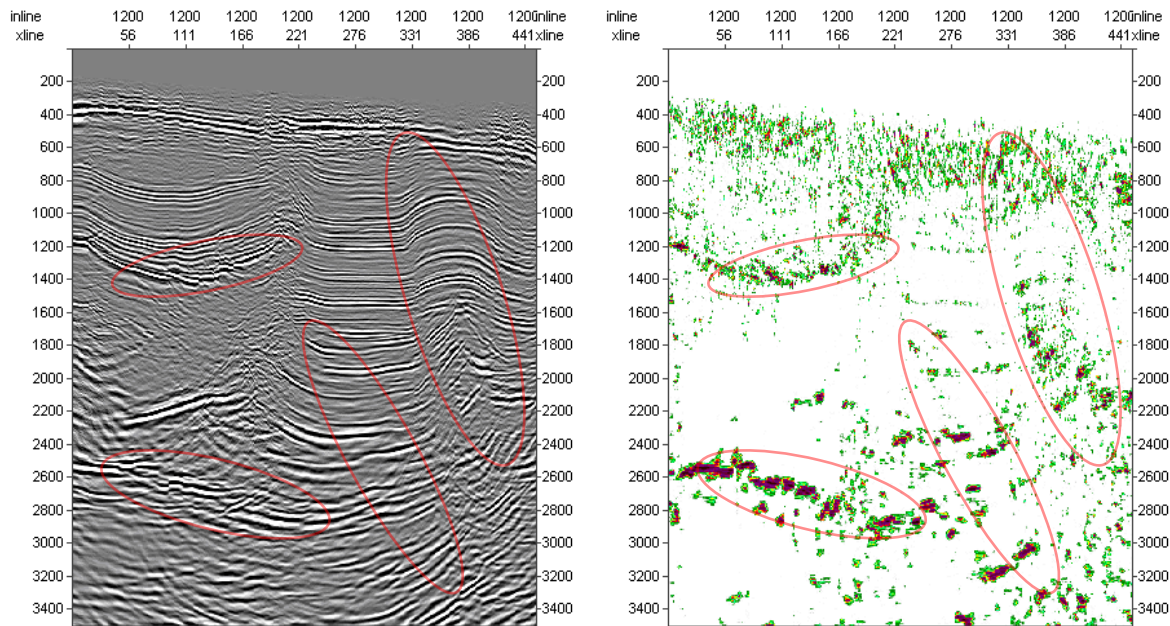


Figure 2. migrated section (b); and diffraction image (c).

References

- Berkovitch, A., Gelchinsky, B., and Keydar, S. [1994] Basic formulae for multifocusing stack. 56th Mtg. Eur. Assoc. Expl. Geophys., Expanded Abstracts, 140.
- Berkovitch, A., Belfer, I., Hassin, I., and Landa, E. [2009] Diffraction imaging by multifocusing. *Geophysics*, 74, WCA75.
- Fomel, S., Landa, E., and Taner, T. [2007] Poststack velocity analysis by separation and imaging of seismic diffractions. *Geophysics*, 72, No 6, 89-94.
- Harlan, W., Claerbaut, J., and Rocca, F. [1984] Signal to noise separation and velocity estimation. *Geophysics*, 49, 1869-1880.
- Hubral, P., Schleicher, J., Tygel, M., and Hanitzsch, C. [1993] Determination of Fresnel zones from traveltme measurements. *Geophysics*, 58, No 6, 703-712.
- Kanasewich, E., and Phadke, S. [1988] Imaging discontinuities on seismic sections. *Geophysics*, 53, 334-345.
- Khaidukov, V., Landa, E., and Moser, T. [2004] Diffraction imaging by focusing-defocusing: An outlook on seismic superresolution. *Geophysics*, 69, 1478-1490.
- Klokov, A., Baina, R., and Landa, E. [2010] Separation and imaging of seismic diffractions in dip angle domain. 72rd EAGE Conference and Exhibition.
- Landa, E., Shtivelman, V., and Gelchinsky, B. [1987] A method for detection of diffracted waves on common-offset sections. *Geophysical Prospecting*, 35, 359-373.
- Landa, E. and Keydar, S. [1998] Seismic monitoring of diffraction images for detection of local heterogeneities. *Geophysics*, 63, No. 3, 1093-1100.
- Moser, T. and Howard C., [2008] Diffraction imaging in depth. *Geophysical Prospecting*, 56, No 5, 627-641.
- Reshef, M. and Landa, E. [2009] Poststack velocity analysis in the dip-angle domain using diffractions. *Geophysical Prospecting*, 57, 811-821.
- Taner, T., Fomel, T., and Landa, E. [2006] Separation and imaging of seismic diffractions using plane-wave decomposition. 76th Annual International Meeting, SEG, Expanded Abstracts, 25, 2401-2405.